



RETROFITTING HOLLOW CONCRETE MASONRY INFILL WALLS USING GLASS FIBER REINFORCED PLASTIC LAMINATES

Zeyad H. R. Hakam¹, Ahmad A. Hamid², Mohamed Elgaaly³

ABSTRACT

Many existing masonry-infilled steel frame buildings do not meet today's seismic design standards. Cracking, spalling, and collapse of infill masonry walls which, in turn, lead to substantial structural damage and even collapse of the bounding steel frame have been reported in areas of moderate to high seismicity. A research program, sponsored by the National Science Foundation, was initiated at Drexel University in order to investigate the effectiveness of using glass fiber reinforced plastic (GFRP) laminates to retrofit hollow concrete masonry infilled structural steel frames and to demonstrate the ability of the proposed technique in improving the seismic performance and the strength and deformation characteristics of the infilled frame system. Selected results of Phase I of this investigation, which focused on the use of GFRP laminates to retrofit hollow masonry assemblages subjected to on-axis and off-axis in-plane compressive loads, are presented in this paper. The laminates altered the failure modes of the masonry assemblages and reduced the variability and anisotropic nature of the masonry. Only marginal strength increase was observed for assemblages which exhibited compression failure modes, while significant increases were observed for those which failed due to shear and/or mortar joint slip.

Key words: concrete masonry, infill walls, infilled steel frames, composite laminates, on/off-axis compression tests, unreinforced masonry, retrofit technique

- 1 Senior Project Controls Engineer, Bechtel Power Corporation, 5275 Westview Drive, Frederick, Maryland, 21703, USA; Email: zhakam@bechtel.com
- 2 Professor, Civil & Architectural Engineering Department, Drexel University, 3141 Chestnut Street, Philadelphia, Pennsylvania, 19104, USA; Email: hamidaa@drexel.edu
- 3 Professor, Civil & Architectural Engineering Department, Drexel University, 3141 Chestnut Street, Philadelphia, Pennsylvania, 19104, USA; Email: elgaalym@drexel.edu

INTRODUCTION AND PROBLEM STATEMENT

Hollow unreinforced masonry (URM) walls are commonly used as partitions within the structural framing of buildings. When the masonry infill wall is built tight to the surrounding frame, it has been firmly established that the infill's presence dramatically alters the load-deflection response of the surrounding frame. Poor, even catastrophic, performance of masonry infilled frame structures was encountered in large seismic events. Justification of such performance included [Mehrabi et al. (1994, 1996), Buonopane et al. (1999), Drysdale et al. (1999)]: (a) alteration of the distribution of lateral loads to different components of the structure, (b) introduction of the short column effect (also known as the knee-braced system), (c) presence of high moments and shear forces in the frame's columns caused by the infill panel bearing against the frame, and (d) presence of nonuniform arrangements of infill walls which alter the stiffness distribution and often result in torsional effects.

In light of the above discussion and the continual upgrade of seismic zones and building codes, there exists a definite need to strengthen existing masonry infilled frame structures, especially those constructed with little or no attention to the role of the masonry infill wall [Hakam (2000)]. Traditional methods of strengthening masonry buildings often entailed the installation of additional stiffening elements, grout injection, the use of external reinforcement such as ferrocement and shotcrete coats, and/or addition of walls/wythe [Kolsch (1998), Triantafillou (1998), Drysdale et al. (1999)]. However, these retrofit methods are often accompanied by undesirable "side effects," notably: addition of significant mass to the structure which results in increased stresses during seismic events, violation of the structure's aesthetic appeal, and are often labor intensive requiring significant workspace and consuming floor space once installed. Therefore, a relatively new retrofit method was investigated in this study. This scheme entails retrofitting the infilled frame system by strengthening the masonry infill wall itself using glass fiber reinforced plastic (GFRP) laminates that are epoxy-adhered to the infill's exterior surfaces. This proposed method alleviates the undesirable side effects of other retrofit methods due to the laminates' remarkable strength-to-weight ratio (thereby adding minimal weight to the structure), ease of application (hence requiring minimal labor and floor space), and proven short-term strength increase (the curing time before full strength is achieved rarely requires more than two or three days) [Hakam (2000)]. It must be emphasized, however, that in light of the relatively recent application of FRP laminates in structural applications, issues pertaining to their long-term strength, creep characteristics, delamination, and environmental concerns (such as exposure to ultraviolet radiation and heat) still need to be established/addressed; these concerns are beyond the scope of this study.

EXPERIMENTAL PHASE I SCOPE OF WORK AND TEST MATRIX

Collapse mechanisms of infilled frames included failure of the infill panel and formation of plastic hinges in the frame columns and/or beams [Liauw et al. (1983a, 1983b), Moghaddam et al. (1987), Saneinejad et al. (1995), Seah (1998)]. Essentially, three failure modes were identified, namely: corner crushing mode (compressive crushing of the infill in at least one of the loaded corners along the diagonal strut), diagonal compression mode (extensive cracking followed by crushing of the central region of the infill), and shear mode (horizontal shear slip along the bed joints of the masonry infill panel). The center of the infill panel is initially subjected to diagonal tension which

causes cracking in the mortar joints and/or masonry units. Thus, it is evident that different regions of the masonry infill panel are subjected to different loading conditions, namely: compression, joint shear, diagonal tension and combinations of normal and shear forces. Consequently, prior to studying steel frames infilled with the retrofitted masonry wall panels, it was imperative to investigate the effect of retrofitting hollow block masonry using GFRP laminates in order to determine the properties and characteristics of this “new” composite material with which the steel frames will be infilled. This constituted the first phase of the experimental program conducted in this study and is the main focus of this paper. This segment served as a prerequisite to the second experimental phase of the study in which moment-resisting, structural steel frames infilled with both unretrofitted and GFRP-retrofitted hollow block masonry walls were tested under in-plane diagonal loading. This latter portion of the experimental program is not the main focus of this paper and is covered elsewhere [refer to Hakam (2000)]. In light of the available testing facilities at the Structural Testing Laboratory of Drexel University, one-third scale testing was selected. Worthy to note is that small-scale modeling and testing techniques have been well established at Drexel University since the late 1970’s.

Thus, simulating the various stresses which URM infill walls are subjected to when confined within structural steel frames, Phase I of the experimental investigation focused on evaluating the effect of GFRP-strengthening of hollow masonry assemblages (i.e. prisms) tested under the following in-plane loading conditions (see Table 1):

1. *On/off-axis compression*: In-plane, concentric, compressive loads were applied at various inclinations with respect to the bed joints, specifically at 90° (normal to the bed joints, also referred to as “on-axis compression”), 0° (parallel to the bed joints), 30°, 45° and 60°. The latter three off-axis compression loading conditions simulate combined normal and shear in-plane stresses resulting from angles corresponding to common aspect ratios of infill walls.
2. *Pure joint shear*: This enabled to evaluate the benefit of GFRP overlays in resisting the traditionally weak and brittle horizontal shear slip failure mode.
3. *Diagonal tension*: This is a standard testing procedure used to evaluate the diagonal tensile (or shear) strength of unreinforced masonry. Again, the impact of GFRP-retrofit was studied.

Additional masonry assemblages, similar to those of Phase I, were built during the construction of the infilled frames of Phase II for the purpose of quality control and were also used to complement the results of Phase I assemblages. These latter prisms, referred to as Phase II assemblages, are not shown in Table 1.

Table 1: Test matrix for the experimental Phase I.

Phase I “Assemblage Testing and Analysis” Test Description		No. of Tests	
		Unretrofitted	Retrofitted
1)	<i>On/Off-Axis Compression Tests (see Note 1):</i>		
(a)	$\theta=90^\circ$ (axial compression normal to bed joints)	3	3
(b)	$\theta=0^\circ$ (axial compression parallel to bed joints)	3	3
(c)	$\theta=45^\circ$	3	3
(d)	$\theta=30^\circ$	3	3
(e)	$\theta=60^\circ$	3	3
2)	<i>Diagonal Tension Test</i>	3	3
3)	<i>Joint Shear Test</i>	3	3

NOTE 1: θ = Angle between direction of compressive load and mortar bed joints.

MATERIAL SELECTION AND CHARACTERISTICS

Since one-third model testing was employed in this study, similitude requirements relating the small-scale model and the prototype structure were obeyed [Harris et al. (1999)]. The following summarizes key mechanical properties and selection criteria for the materials used in Phase I of this study.

Masonry Blocks and Mortar

One-third scale, hollow concrete masonry units replica of the standard, full-scale, ASTM C 90-92b, 150 mm (6 in.) wide, two core, hollow block were manufactured using the small-scale block-making machine at Drexel University. The average net-area-based compressive strength of the blocks was 27.62 MPa (4,006 psi) within a coefficient of variation of 17.04%. The masonry assemblages and walls were constructed using scaled down mortar joints with a nominal thickness of 3.2 mm ($\frac{1}{8}$ in.). To simulate actual construction practice, the mortar mix was designed as Type S mortar and all mortar joints were tooled to a concave profile. The average compressive strength of 50 mm (2 in.) cube samples taken during the construction of the assemblages of Phase I was 25.19 MPa (3,653 psi) within a coefficient of variation of 5.40%.

GFRP Laminates

FRP composite laminates can contain fibers made of carbon, aramid or glass; thus, they vary in their tensile strength, deformation characteristics and cost. Laminates made of E-glass fibers, being the most widely used in construction, were used in this study. In light of the symmetric nature of the diagonal testing of the infilled frames of Phase II and the fact that the infill walls had an aspect ratio (height-to-length) of unity, it was decided to use bi-directional lamina composed of equal amounts of fibers weaved at right angles to each other. In order to select a GFRP laminate product suitable for retrofitting the one-third scale URM walls, an equivalent-stiffness-based approach was used to determine the laminate thickness and number of plies (i.e. layers) which correspond to the requirement of the Masonry Standards Joint Committee (MSJC) code stipulating that infill and partition masonry walls in high seismic zones be reinforced in the vertical and horizontal directions with a minimum steel reinforcement ratio of 0.2% of the gross cross-sectional area of the wall [MSJC (1999)]. In other words, an area of laminate reinforcement equivalent to the stipulated area of steel reinforcement was calculated using the modular ratio of the steel to the GFRP laminate.

The selected GFRP laminate was obtained from Fyfe Co. LLC “The Fibrwrap® Company,” San Diego, California [Fyfe Co. (1998)]. This product is available under the brand name “Tyfo® WEB Fabric and Tyfo® Hi-Clear Epoxy.” The selected overlay consists of a white colored fabric made of continuous E-glass fibers whose ultimate tensile strength is 1,516.8 MPa (220 ksi). Upon adhering the fabric to the surface of the masonry using a specified epoxy resin, a clear (almost transparent) laminate with a shiny hue is produced. The nominal or “design” thickness of the laminate is 0.4 mm (0.014 in.) per lamina or ply [Fyfe Co. (1998)]. Table 2 summarizes the results of the supplier-furnished in-plane tensile tests in the direction(s) parallel to the fiber orientations in accordance with ASTM D 3039/D 3039M-93 standard specification. However, it should be noted that, for design purposes, the supplier recommends the use of lower-bound

values of 206.8 MPa (30 ksi) and 1.5% for the tensile ultimate strength and strain respectively. Along directions parallel to the fiber orientations, a linear stress-strain relationship exists until failure. Based on the aforementioned equivalent stiffness based selection criterion, it was decided to apply one ply of the laminate on each face of the URM masonry walls being retrofitted.

Table 2: Results of GFRP laminate tensile tests performed by the supplier.

Description	Average Value	Sample Standard Deviation	Coeff. of Variation
Ultimate Strength	311.81 MPa (45.224 ksi)	33.09 MPa (4.800 ksi)	10.61%
Ultimate Strain	1.66% = 0.0166	0.0017	10.02%
Modulus of Elasticity	19.92 GPa (2.89x10 ⁶ psi)	1.83 GPa (0.27x10 ⁶ psi)	9.20%

Construction and Test Setup of On/Off-Axis Compression Assemblages

In this series of tests, the angle between the in-plane compressive load direction and the masonry assemblage's bed joint direction, denoted as " θ ," was varied as the test parameter. Five values of θ were experimentally investigated, namely: 90°, 0°, 30°, 45°, and 60°. A special case of the off-axis compression tests is when the applied load is normal to the bed joints, i.e. $\theta=90^\circ$ (also referred to as "on-axis compression"), and is the usual direction for which load bearing masonry is designed to resist loads. The 90° assemblages were constructed as four-unit high, one-block wide prisms and were tested in accordance with ASTM E 447-92b (see Figure 1).

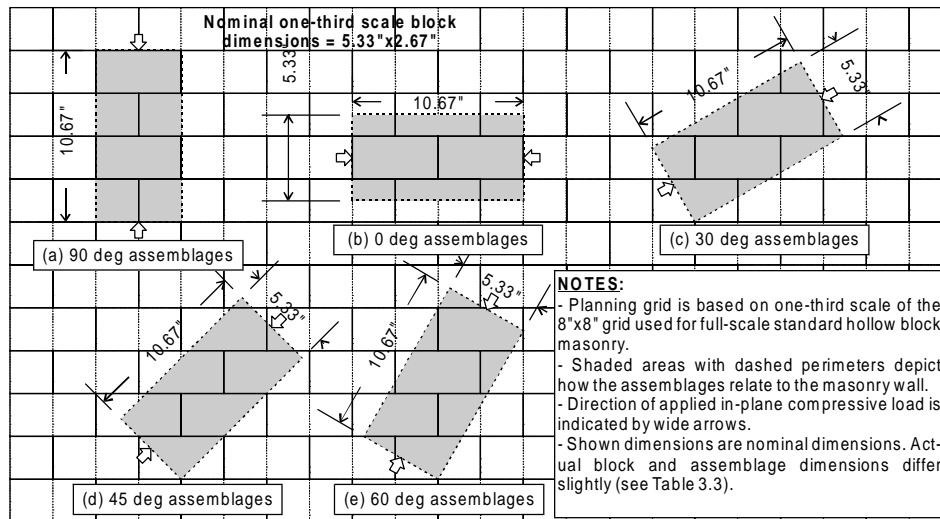


Figure 1: On/off-axis compression assemblages.

As the modular planning grid shown Figure 1 illustrates, the different assemblages were of similar dimensions in order to permit comparison of their failure loads. Since it was not feasible to "cut" the 0°, 30°, 45° and 60° assemblages from masonry walls, the individual blocks for each assemblage were initially cut to shape using a masonry saw. Then, simulating actual construction, wooden forms inclined at various angles were built

in order to lay the pre-cut blocks in the normal upright position with the bed and head joints being horizontal and vertical respectively (see Figure 2). After air-curing for at least 28 days, half of the constructed specimens were retrofitted using the GFRP laminates. The laminates were installed using a typical hand lay-up process in which a first coat of epoxy was applied to the masonry surface using a paint roller after which the fabric was adhered such that the fibers run parallel and normal to the bed joints, and then a final coat of epoxy was applied. All assemblages were tested in accordance with the ASTM E 477-92 specification. The test setup is illustrated in Figure 3. The gypsum-capped assemblages were instrumented using two pairs of linear variable differential transducers (LVDTs) to measure compressive deformations along the direction of the applied compressive load.

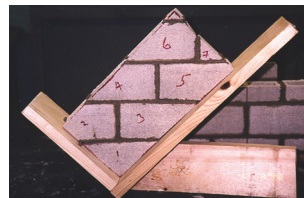


Figure 2: Completed 45° assemblage left to cure at air temperature while resting on its wooden formwork.

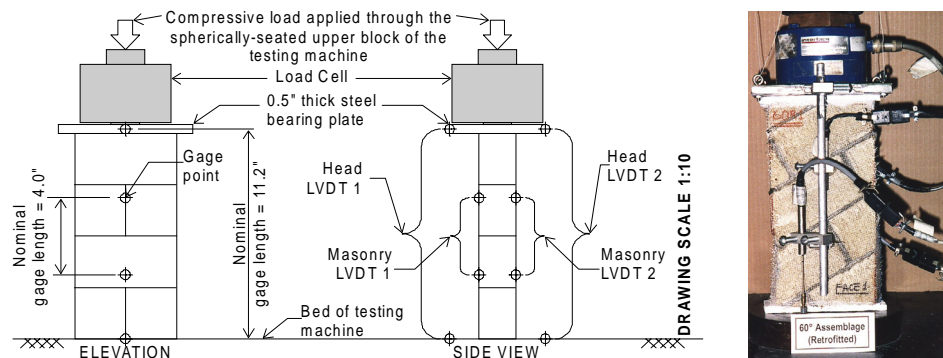


Figure 3: Gage points and LVDT locations for on/off-axis compression assemblages.

Summary of Test Results

Details of the individual tests and corresponding results for each on/off-axis compression assemblage are reported in Hakam (2000). The following summarizes key test results and pertinent observations.

Failure Modes

As expected, the unretrofitted on/off-axis compression assemblages exhibited varying failure modes depending on the angle of the applied in-plane compressive load. The 0° and 90° assemblages exhibited typical compression failure modes characterized by vertical splitting along the webs and the face shells similar to that observed in full-scale prototype masonry prisms reported in the literature [Hamid (1978), Drysdale et al. (1999)]. This vertical tensile splitting is attributed to the lateral stresses which developed in the blocks due to the varying lateral stress profile along the height of the assemblage caused by the different lateral strain characteristics of the mortar and the blocks. For the

unretrofitted 30° assemblages, pure joint shear slip failure was observed due to the dominance of the shearing component of the applied load along the bed joint as opposed to the normal compressive component. Similarly, the 45° assemblages also failed by pure joint shear slip along the middle bed joint although some hairline cracking was also observed in the off-center bed joints. Finally, the unretrofitted 60° assemblages failed in a combined failure mode with cracks extending through the blocks and along the mortar joints. Noticeably, all failure modes were brittle and the assemblages disintegrated almost immediately after attainment of the maximum load. Figure 4 illustrates the encountered failure modes for the unretrofitted assemblages.

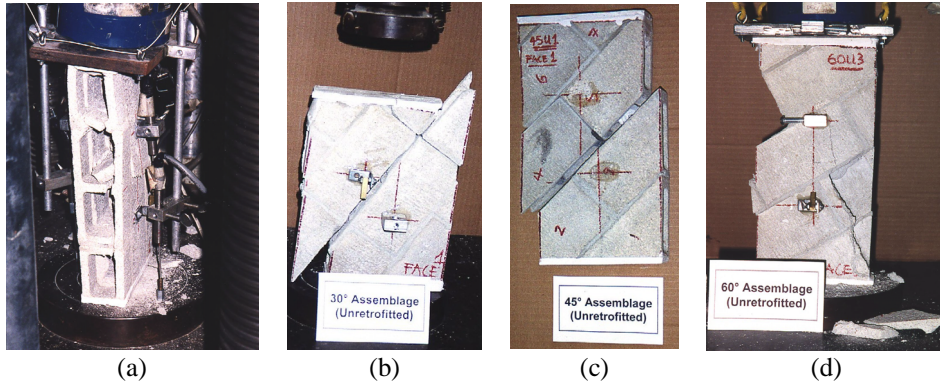


Figure 4: Failure modes of the unretrofitted on/off-axis compression assemblages: (a) vertical tensile splitting through the webs in the 0° and 90° assemblages (0° assemblage shown), (b) pure joint slip failure in a 30° assemblage, (c) pure joint slip failure in a 45° assemblage, and (d) combined failure in a 60° assemblage.



(a) Vertical tensile splitting through the webs (90° assemblage shown).



(b) Upon load removal, all webs were damaged leaving two standing face shells.



(c)
Similar failure mode in 0° assemblages.



(d)
Similar failure in a 60° assemblage.

Figure 5: Failure mode of the retrofitted on/off-axis compression assemblages

In contrast, all retrofitted on/off-axis compression assemblages exhibited one failure mode which was vertical splitting of the interior webs. The typical retrofitted assemblage was reduced to two intact face shell subassemblages with all interior webs damaged (see Figure 5 above). For the 30° and 45° assemblages, some signs of laminate stretching or minor delamination along the bed joints were observed. This failure mode confirms the role of the laminate in reducing the anisotropy of the masonry and effectively reinforcing the planes of weakness (being the mortar head and bed joints). Consequently, failure occurred in the “new” weak elements of the assemblages which are the webs since they are essentially the only part not retrofitted by virtue of their interior location.

Failure Loads and Moduli of Elasticity

Table 3 and corresponding Figure 6 portray the variation of the compressive strengths of the unretrofitted versus retrofitted assemblages of Phase I. For comparative purposes, the compressive strengths of the assemblages were calculated as the maximum load-carrying capacity divided by the gross assemblage area perpendicular to the direction of the applied load. It is clear that, while the failure loads of the unretrofitted assemblages varied widely depending on their failure mode, those of the retrofitted assemblages did not vary significantly. Moreover, the fact that the values of the coefficients of variation for the retrofitted assemblages are generally lower than those of the unretrofitted specimens is further evidence of the laminate’s role in reducing the inevitable variations in unreinforced masonry construction [Hakam (2000)].

Table 3: Summary of the compressive strengths of the on/off-axis compression assemblages.

ASSEMBLAGE TYPE	UNRETROFITTED			RETROFITTED			STRENGTH INCREASE (X'S)
	Average ⁽¹⁾		Coeff. of Variation	Average ⁽¹⁾		Coeff. of Variation	
	psi	MPa		psi	MPa		
90°	785 ⁽²⁾	5.41 ⁽²⁾	13.8% ⁽²⁾	1,593	10.98	10.9%	2.03
60°	608	4.19	6.1%	1,232	8.49	4.8%	2.03
45°	342	2.36	26.7%	1,414	9.75	6.7%	4.13
30°	265	1.83	14.2%	1,499	10.34	10.3%	5.65
0°	1,039	7.16	15.6%	1,691	11.66	4.5%	1.63

Notes: (1) Based on gross assemblage area of 64.31 cm² (9.969 in²).

(2) Phase I assemblage test results only.

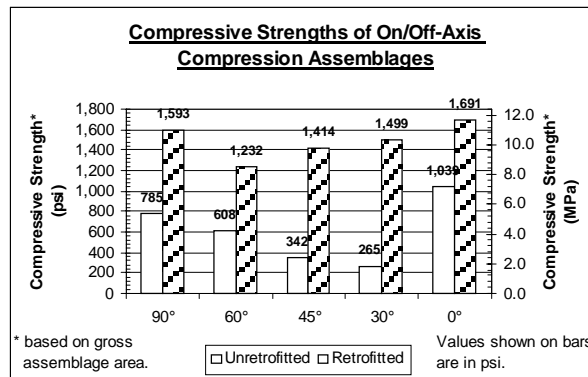


Figure 6: Compressive strengths of the on/off-axis compression assemblages

Compared to the unretrofitted counterparts, the strength increase due to retrofit with the GFRP laminates was greatest for the assemblages which encountered shear slip failure modes; specifically, the 30° and 45° assemblages exhibited strength increases of 5.65 and 4.13 times respectively. On the other hand, the strength contribution was least for the assemblages whose unretrofitted failure mode was strictly compression-related and characterized by vertical web splitting, namely the 0° and 90° assemblages. It is imperative to note that even though the 90° assemblages shown in the table indicate a strength increase of 2.03 times compared to the unretrofitted Phase I specimens, this increase is reduced to only 1.19 times should the average unretrofitted compressive strength of 9.22 MPa (1,337 psi) for Phase II assemblages be used. This difference is discussed in further detail in Hakam (2000). The 60° assemblages exhibited an intermediate strength increase of 2.03 times their unretrofitted counterparts. The greater the in-plane shear stresses along the bed joints are, the greater the contribution of the laminates is in terms of strength increase. This is understandable since the tensile strength of the laminates is significant whereas their compressive strength is negligible [Hakam (2000)].

Table 4: Summary of the moduli of elasticity of the on/off-axis compression assemblages.

ASSEMBLAGE TYPE	UNRETROFITTED			RETROFITTED			PERCENT-AGE INCREASE
	Average		Coeff. of Variation	Average		Coeff. of Variation	
	Ksi	GPa		ksi	GPa		
90° ⁽¹⁾	1,640	11.31	27.1%	1,690	11.65	21.2%	3.1%
60°	1,489	10.27	4.7%	1,609	11.09	9.8%	8.0%
45°	1,461	10.07	26.4%	1,531	10.56	11.8%	4.8%
30°	1,607	11.08	17.4%	1,767	12.18	2.3%	9.9%
0° ⁽¹⁾	1,829	12.61	15.6%	1,958 ⁽²⁾	13.50 ⁽²⁾	10.8% ⁽²⁾	7.0%

Notes: (1) Includes results of Phase I and Phase II assemblage tests.
(2) Modulus of elasticity taken between 5% and 30% of maximum stress instead of 5% and 33% like all other values.

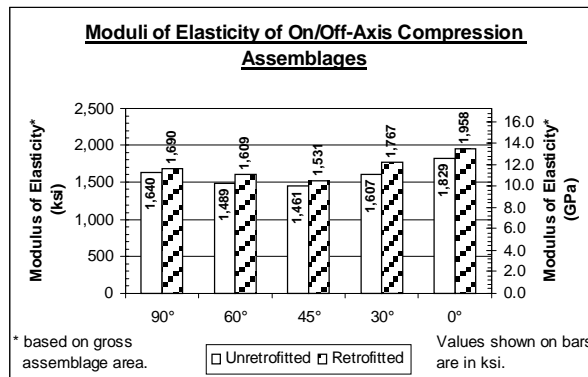


Figure 7: Moduli of elasticity of the on/off-axis compression assemblages

Utilizing plots of the compressive stress versus strain along the direction of the applied load for each assemblage to compute the corresponding initial modulus of elasticity (taken as the chord modulus between 5% and 33% of the assemblage’s compressive strength), the average elasticity moduli and corresponding variation coefficients are summarized in Table 4 and illustrated in Figure 7. To permit comparison, the shown moduli are based on the gross assemblage area. The increase in moduli of the retrofitted assemblages compared to their unretrofitted counterparts is notably less than the compressive strength increase. This indicates that the effect of the laminates on the stiffness of the assemblages is negligible. It should be noted, however, that this observation is based on the relation between the vertical compressive stress and corresponding strain at the early loading stages. A significant contribution of the laminates is in the post-peak behavior. As evidenced in the stress versus strain curves, the retrofitted assemblages did not lose all their strength nor disintegrate upon reaching the maximum strength. In fact, in the majority of the tests, a plateau region was attained during which the compressive stress almost stabilized and began to slowly decrease. Such plateau can be regarded as residual strength after failure of the masonry- a feature which is absent in the case of unreinforced masonry.

A plot of the average compressive strengths versus load orientation with respect to the bed joints is shown in Figure 8. The plot for the unretrofitted assemblages concurs with established notion that the compressive strength of the unreinforced masonry is sensitive to the load orientation [Hamid (1978), Hamid et al. (1981, 1982), Drysdale et al. (1999)]. It should be noted that due to the considerable difference between the average compressive strengths of the unretrofitted 90° assemblages constructed during Phase I and Phase II of this study, two values are shown on the graph. (other tests repeated in both phases, namely the unretrofitted 0° assemblages and the retrofitted 90° and 0° assemblages, yielded comparable strengths). Hamid (1978) tested off-axis compression assemblages at θ values of 15° and 75° in lieu of the 30° and 60° tests adopted in this study. Based on the work by Hamid (1978), it is likely that the variation of the compressive strength between 0° and 30° is considerably steeper than that shown by the original curve. The probable variation of compressive strength between $\theta=0^\circ$ and $\theta=30^\circ$ is indicated by the dashed line labeled “Suggested Path” in Figure 8.

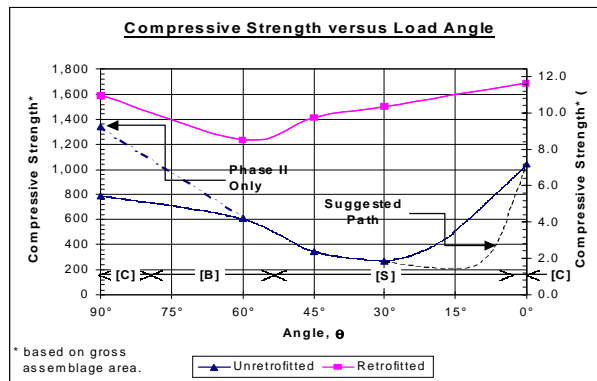


Figure 8: Compressive strength versus load orientation with respect to the bed joints

Based on the failure hypothesis for hollow block masonry proposed by Hamid et al. (1981) and in view of the test results herein, the shown curve for unretrofitted assemblages incorporates three different failure modes which can be summarized as one of the following: (1) Shear failure along the bed joint which is primarily encountered at low values of θ which are greater than 0° and up to approximately 45° , (2) Compression failure and vertical splitting which is the characteristic failure mode of the 0° and 90° assemblages (and at nearby angles), and (3) Combined failure characterized by cracking through the blocks and along the mortar head and bed joints, occurring between 45° and 90° . The above three modes are illustrated in Figure 8 as zones designated as “[S],” “[C]” and “[B]” respectively. On the other hand, the trend line for retrofitted assemblages is considerably “flatter,” thereby indicative of the independence of the compressive strength of the retrofitted masonry from the orientation of the applied load with respect to the bed joints. As discussed earlier, the failure mode of all the retrofitted on/off-axis assemblages was similar and featured splitting through the webs. The inclination of the webs and inevitable material variation (such as initial cracks) are probable causes of the trend line not being completely flat.

CONCLUSIONS

An extensive study was undertaken at Drexel University, Philadelphia, Pennsylvania, to investigate the feasibility and effectiveness of retrofitting hollow concrete masonry infilled structural steel frames through the indirect strengthening of the masonry infill walls by adhering glass fiber reinforced plastic (GFRP) laminates. In the first phase of the experimental investigation, various unretrofitted and GFRP-retrofitted masonry assemblages were tested under a variety of in-plane lateral loads which simulate the various loading conditions that different regions of a typical infill panel are subjected to. In particular, a series of on/off-axis compression tests in which identically sized masonry assemblages were subjected to concentric, in-plane compressive loads at various load orientations with respect to the bed joints demonstrated the beneficial contribution of the GFRP laminate retrofit. Contrary to the unretrofitted assemblages which exhibited varying failure modes such as vertical web splitting, joint shear slip or combined failure modes, the retrofitted assemblages all failed in one manner characterized by vertical web splitting. While the interior webs of the retrofitted assemblages were damaged, minimal distress was observed in the exterior face shells. Moreover, for the assemblages which

failed in typical compression modes, the increase in load carrying capacity was minimal whereas significant increases were realized in the assemblages which primarily failed in tensile or shear slip modes. The GFRP laminates clearly reduced the anisotropy of unreinforced masonry.

ACKNOWLEDGEMENTS

The work presented here constitutes a portion of the doctoral thesis of the first author, Hakam [2000]. The National Science Foundation, US, is acknowledged for sponsoring this research project (grant number CMS-9730646) which was conducted at Drexel University, Philadelphia, PA. Thanks are also due to Fyfe Co. LLC "The Fibrwrap® Company," San Diego, California, who donated the GFRP material used in this project and to D. M. Sabia Company, Inc., Conshohocken, Pennsylvania, for donating the mason time.

REFERENCES

- American Society for Testing and Materials, ASTM C 90-92b, "Standard Specification for Load-Bearing Concrete Masonry Units," Annual Book of ASTM Standards, Vol. 04.05, West Conshohocken, Pennsylvania.
- American Society for Testing and Materials, ASTM E 447-92b, "Standard Test Methods for Compressive Strength of Masonry Prisms," Annual Book of ASTM Standards, Vol. 04.05, West Conshohocken, Pennsylvania.
- Buonopane, S. G. and White, R. N. (1999) "Pseudodynamic Testing of Masonry Infilled Reinforced Concrete Frame," *Journal of Structural Engineering*, ASCE, Vol. 125, No. 6, June, pp. 578-589.
- Drysdale, R. G., Hamid, A. and Baker L. R. (1999) "Masonry Structures: Behavior and Design," second edition, The Masonry Society, Boulder, Colorado.
- Fyfe Co. (1998) "TYFO® Systems for Unreinforced Masonry and Reinforced Concrete/Masonry Wall Strengthening," product brochure, FyFe Co. LLC "The Fibrwrap® Company," San Diego, CA, July.
- Hakam, Zeyad H. R. (2000) "Retrofit of Hollow Concrete Masonry Infilled Steel Frames Using Glass Fiber Reinforced Plastic Laminates," Ph. D. thesis, Civil and Architectural Engineering Department, Drexel University, Philadelphia, Pennsylvania, June.
- Hamid, A. A. A. (1978) "Behavior Characteristics of Concrete Masonry," Ph.D. thesis, McMaster University, Ontario, Canada, September.
- Hamid, A. A. and Drysdale, R. G. (1981) "Proposed Failure Criteria for Concrete Block Masonry under Biaxial Stresses," *Journal of the Structural Division*, Proceedings of the American Society of Civil Engineers, Vol. 107, No. ST8, August, pp. 1675-1687.
- Hamid, A. A. and Drysdale, R. G. (1982) "Proposed Failure Criteria for Brick Masonry under Combined Stresses," Proceedings of the Second North American Masonry Conference, August, pp. 9-1 to 9-11.
- Harris, H. G. and Sabnis, Gajanan M. (1999) "Structural Modeling and Experimental Techniques," second edition, CRC Press, New York.

- Kolsch, H. (1998) "Carbon Fiber Cement Matrix (CFCM) Overlay System for Masonry Strengthening," *Journal of Composites for Construction*, ASCE, Vol. 2, No. 2, May, pp. 105-109.
- Liauw, T. C. and Kwan, K. H. (1983a) "Plastic Theory of Non-integral Infilled Frames," *Proceedings of the Institution of Civil Engineers, Part 2*, Vol. 75, September, pp. 379-396.
- Liauw, T. C. and Kwan, K. H. (1983b) "Plastic Theory of Infilled Frames with Finite Interface Shear Strength," *Proceedings of the Institution of Civil Engineers, Part 2*, Vol. 75, December, pp. 707-723.
- Masonry Standards Joint Committee (MSJC, 1999a) "Building Code Requirements for Masonry Structures (ACI 530-99/ASCE 599/ TMS 402-99)," reported by the Masonry Standards Joint Committee.
- Mehrabi, A. B., Shing, P. B., Schuller, M. P. and Noland, J. L. (1996) "Experimental Evaluation of RC Frames," *Journal of Structural Engineering*, ASCE, Vol. 122, No. 3, March, pp. 228-237.
- Mehrabi, A. B., Shing, P. B., Schuller, M. P. and Noland, J. L. (1994) "Performance of Masonry-Infilled R/C Frames under In-Plane Lateral Loads," Rep. CU/SR-94-6, Dept. of Civil, Environmental, and Architectural Engineering, Univ. of Colorado at Boulder, Colorado, October.
- Moghaddam, H. A. and Dowling, P. J. (1987) "The State of the Art in Infilled Frames," ESEE Research Report No. 87-2, Civil Engineering Department, Imperial College of Science and Technology, August.
- Saneinejad, A. and Hobbs, B. (1995) "Inelastic Design of Infilled Frames," *Journal of Structural Engineering*, ASCE, Vol. 121, No. 4, April, pp. 634-650.
- Seah, C. K. (1998) "A Universal Approach for the Analysis and Design of Masonry Infilled Frame Structures," Ph.D. thesis, The University of New Brunswick, Canada, December.
- Triantafillou, T. C. (1998) "Strengthening of Masonry Structures using Epoxy-Bonded FRP Laminates," *Journal of Composites for Construction*, ASCE, Vol. 2, No. 2, May, pp. 96-104.